

New Pathways for Chlorine Dioxide Decomposition in Basic Solution

Ihab N. Odeh, Joseph S. Francisco, and Dale W. Margerum*

Department of Chemistry, Purdue University, West Lafayette, Indiana 47907-1393

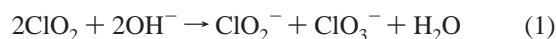
Received July 19, 2002

The product distribution from the decay of chlorine dioxide in basic solution changes as the ClO_2 concentration decreases. While disproportionation reactions that give equal amounts of ClO_2^- and ClO_3^- dominate the stoichiometry at millimolar or higher levels of ClO_2 , the ratio of ClO_2^- to ClO_3^- formed increases significantly at micromolar ClO_2 levels. Kinetic evidence shows three concurrent pathways that all exhibit a first-order dependence in $[\text{OH}^-]$ but have variable order in $[\text{ClO}_2]$. Pathway 1 is a disproportionation reaction that is first order in $[\text{ClO}_2]$. Pathway 2, a previously unknown reaction, is also first order in $[\text{ClO}_2]$ but forms ClO_2^- as the only chlorine-containing product. Pathway 3 is second order in $[\text{ClO}_2]$ and generates equal amounts of ClO_2^- and ClO_3^- . A Cl_2O_4 intermediate is proposed for this path. At high concentrations of ClO_2 , pathway 3 causes the overall ClO_3^- yield to approach the overall yield of ClO_2^- . Pathway 2 is attributed to OH^- attack on an oxygen atom of ClO_2 that leads to peroxide intermediates and yields ClO_2^- and O_2 as products. This pathway is important at low levels of ClO_2 .

Introduction

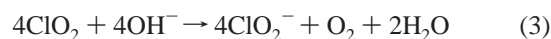
Recent use of chlorine dioxide for the disinfection of anthrax-contaminated premises¹ as well as its growing use in water disinfection,² wastewater treatment,³ pulp bleaching,⁴ chemosterilization,⁵ and food preservation⁶ shows the need for a better understanding of the chemical reactions of this free radical. The rate of decomposition of ClO_2 in neutral aqueous solutions is quite slow,⁷ but its decay is accelerated by base.⁸ The disproportionation reaction in eq 1 has been proposed by many investigators.^{8–13} Bray⁸ proposed a third-order rate expression for this disproportionation (eq 2) with a rate constant of $15.3 \text{ M}^{-2} \text{ s}^{-1}$ at 19°C . Halperin and Taube⁹ studied the general features of ClO_2 decay in base with ^{18}O -labeling techniques at millimolar ClO_2 levels and concluded that a dimer, Cl_2O_4 , forms which subsequently reacts with

OH^- . Disproportionation rate expressions with both a first-order and a second-order dependence in ClO_2 concentration have been cited several times.^{10–13} However, the rate constants are not in agreement and it is not clear how the kinetic data were fit to the rate expression.



$$-\frac{d[\text{ClO}_2]}{dt} = k[\text{OH}^-][\text{ClO}_2]^2 \quad (2)$$

In this work we show that an integrated rate expression can be used to determine reliable first-order and second-order rate constants for the mixed-order decay of ClO_2 over a wide concentration range. Furthermore, we show that at low ClO_2 concentrations the yield of ClO_2^- is greater than the yield of ClO_3^- . We attribute this behavior to the presence of the decay reaction in eq 3, where ClO_2 oxidizes the solvent. The mixed-order integrated rate expression and the use of ion chromatographic measurements of ClO_2^- and ClO_3^- yields permit the identification of three pathways for the decay of ClO_2 . The reaction orders and product yields are different for the proposed pathways, but all three mechanisms have base-assisted electron-transfer steps.¹⁴



* To whom correspondence should be addressed. E-mail: margerum@chem.purdue.edu.

- (1) Ritter, S. K. *Chem. Eng. News* **2001**, 79 (48), 24–26.
- (2) Katz, A.; Narkis, N. *Wat. Res.* **2001**, 35, 101–108.
- (3) Stevens, A. A. *Environ. Health Perspect.* **1982**, 46, 101–110.
- (4) Hart, P. W.; Hsieh, J. S. *Chem. Eng. Commun.* **1993**, 126, 27–41.
- (5) Rosenblatt, D. H. U.S. Patent 4 504 442, 1983.
- (6) Tsai, L. S.; Huxsoll, C. C.; Roberston, G. J. *Food Sci.* **2001**, 66, 472–477.
- (7) Von Heijne, G.; Teder, A. *Acta Chem. Scand.* **1973**, 27, 4018–4019.
- (8) Bray, W. C. Z. *Anorg. Allg. Chem.* **1906**, 48, 217–250.
- (9) Halperin, J.; Taube, H. *J. Am. Chem. Soc.* **1952**, 74, 375–380.
- (10) Granstrom, M. L.; Lee, G. F. *Public Works* **1957**, 88, 90–92.
- (11) Gordon, G.; Keiffer, R. G.; Rosenblatt, D. H. In *Progress in Inorganic Chemistry*; Lippard, S. J., Ed.; Wiley-Interscience: New York, 1972; pp 201–287.
- (12) Emerich, D. E. Ph.D. Dissertation, Miami University, 1981.
- (13) Gordon, G. *Pure Appl. Chem.* **1989**, 61, 873–878.

- (14) Wang, L.; Nicoson, J. S.; Huff Hartz, K. E.; Francisco, J. S.; Margerum, D. W. *Inorg. Chem.* **2002**, 41, 108–113.

Experimental Section

Reagents. All solutions were prepared with doubly deionized, distilled water. Chlorine dioxide was prepared as described elsewhere¹⁴ and was protected from light and stored in a refrigerator. The stock ClO₂ solution was standardized spectrophotometrically at 359 nm ($\epsilon = 1230 \text{ M}^{-1} \text{ cm}^{-1}$).¹⁵ Commercially available NaClO₂ was recrystallized using a previously described procedure,¹⁶ and its purity was determined by ion chromatography. Stock solutions of NaClO₂ were standardized spectrophotometrically at 260 nm ($\epsilon = 154.0 \text{ M}^{-1} \text{ cm}^{-1}$).¹⁵ Ionic strength, μ , was adjusted to 1.0 M with recrystallized NaClO₄.

pH Measurement. An Orion model 720A digital pH meter equipped with a Corning combination electrode was used for pH measurements. The electrode was calibrated with previously standardized HClO₄ and NaOH to correct pH to $p[\text{H}^+]$ when pK_w is 13.60 (25.0 °C, 1.0 M NaClO₄).¹⁷

Kinetics. Kinetic traces for ClO₂ decay in base were acquired with a Perkin-Elmer Lambda 9 UV-vis-NIR spectrophotometer. The kinetics of the ClO₂ reaction with HO₂⁻ were followed by use of an Applied PhotoPhysics SX18 MV stopped-flow spectrophotometer (APPSF, optical path length = 0.962 cm). These reactions were followed by measuring the loss of ClO₂ at 359 nm. SigmaPlot 8.0¹⁸ was used for regression analyses.

Product Analysis. A Dionex DX-500 chromatograph was used to measure yields of ClO₂⁻ and ClO₃⁻ by a method similar to EPA 300.1.¹⁹ Samples were injected via an autosampler (AS 40) through a 25 μL injection loop onto quaternary amine anion-exchange guard (AG9 HC) and separation (AS9 HC) columns. Analytes were eluted with 9 mM Na₂CO₃ at a flow rate of 1.0 mL/min. Gas-assisted suppressed-conductivity detection (ED 40), with an ASRS-Ultra suppressor in the self-regenerating mode and a current of 100 mA, was used to detect the analytes. Residual ClO₂ was purged with Ar prior to injection onto the column. Ionic strength was not adjusted in the stoichiometric analyses. The use of polypropylene as opposed to glass containers¹² and alternative preparation methods of ClO₂ synthesis²⁰ did not affect the product distribution.

Computation. Calculations were performed using the GAUSSIAN 98 program²¹ to determine plausible structures for the reaction intermediates. Equilibrium geometries were optimized using the Becke three-parameter hybrid functional combined with the Lee, Yang, and Parr correlation (B3LYP) density functional theory method. Initial geometry optimizations were done at the B3LYP level of theory using the 6-311G(d) basis set. The calculations with the large 6-311++G(3df,3pd) basis set were also performed and included. All equilibrium geometries were fully optimized to better than 0.001 Å for bond distances and 0.1° for bond angles. All energies were corrected for zero-point energies as determined from harmonic vibrational frequency calculations.

Results and Discussion

Kinetics. The decay of ClO₂ in basic solution (with excess [OH⁻]) does not fit the second-order dependence in [ClO₂] that is given in eq 2, nor does it fit a simple first-order dependence in [ClO₂]. As shown in Figure 1, the decay fits

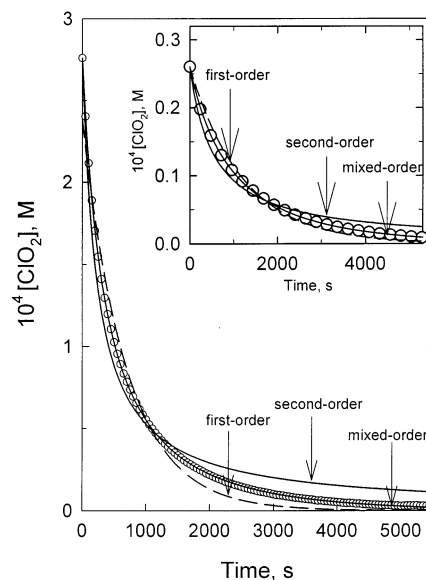


Figure 1. Kinetic trace and regression results for the decomposition of ClO₂ in basic solution. Conditions: 0.37 mM ClO₂; 0.40 M NaOH; 25.0–(2) °C; $\mu = 1.0 \text{ M}$. Circles are the experimental data. The mixed-order dependence in [ClO₂] regression line is based on eq 5. Insert shows the decomposition of ClO₂ at 25 μM levels, with all other conditions as above (circles). The mixed-order fit is obtained using eq 5. $k_{a,\text{obsd}} = 6.19(3) \times 10^{-4} \text{ s}^{-1}$, and $k_{b,\text{obsd}} = 8.28(3) \text{ M}^{-1} \text{ s}^{-1}$.

a mixed-order (combination of first-order and second-order) dependence in [ClO₂] as given in eq 4. This is the case over a wide range of ClO₂ concentrations (see insert of Figure 1). An integrated rate expression (eq 5) gives excellent fits for all the kinetic data, where [ClO₂]₀ is the initial concentration of ClO₂ and [ClO₂]_t is the concentration of ClO₂ at any time during the course of the reaction.

$$-\frac{d[\text{ClO}_2]}{dt} = k_{a,\text{obsd}}[\text{ClO}_2] + k_{b,\text{obsd}}[\text{ClO}_2]^2 \quad (4)$$

$$[\text{ClO}_2]_t = \frac{k_{a,\text{obsd}}[\text{ClO}_2]_0 e^{-k_{a,\text{obsd}}t}}{k_{a,\text{obsd}} + k_{b,\text{obsd}}([\text{ClO}_2]_0 - [\text{ClO}_2]_0 e^{-k_{a,\text{obsd}}t})} \quad (5)$$

This expression permits resolution of $k_{a,\text{obsd}}$ and $k_{b,\text{obsd}}$ values as the OH⁻ concentration varies from 0.05 to 0.45 M (Figure 2) and shows that there is a first-order dependence in [OH⁻] for both $k_{a,\text{obsd}}$ and $k_{b,\text{obsd}}$ (eq 6). The resolved values are $k_a = 1.38(8) \times 10^{-3} \text{ M}^{-1} \text{ s}^{-1}$ and $k_b = 21.8(4) \text{ M}^{-2} \text{ s}^{-1}$ at 25.0 °C, $\mu = 1.0 \text{ M}$. The k_a value is a factor of 2.3 smaller and the k_b value is 1.3 larger than the corresponding values of Granstrom and Lee.¹⁰ However, our stoichiometric studies show that k_a represents two first-order pathways rather than one. The data show, as will be detailed later, that ClO₂ decomposition proceeds by three concurrent pathways.

$$-\frac{d[\text{ClO}_2]}{dt} = k_a[\text{OH}^-][\text{ClO}_2] + k_b[\text{OH}^-][\text{ClO}_2]^2 \quad (6)$$

Stoichiometry. Ion chromatography shows that ClO₂⁻ and ClO₃⁻ are the only chlorine-containing products formed from the decomposition of ClO₂ in basic solution. However, the ratio of ClO₂⁻ to ClO₃⁻ is not 1:1 as required for the disproportionation reaction (eq 1) and reported by several

(15) Furman, C. S.; Margerum, D. W. *Inorg. Chem.* **1998**, *37*, 4321–4327.

(16) Jia, Z.; Margerum, D. W.; Francisco, J. S. *Inorg. Chem.* **2000**, *39*, 2614–2620.

(17) Molina, M.; Melios, C.; Tognolli, J. O.; Luchiani, L. C.; Jafelicci, M. *J. Electroanal. Chem. Interfacial Electrochem.* **1979**, *105*, 237–246.

(18) *SigmaPlot 8.0 for Windows*; SPSS Inc.: Chicago, IL, 2002.

(19) *EPA Method 300.1*; U.S. EPA: Cincinnati, OH, 1997.

(20) Granstrom, M. L.; Lee, G. F. *J. AWWA* **1958**, *50*, 1453–1466.

(21) Frisch, M. J.; et al. *GAUSSIAN 98*; Gaussian Inc.: Pittsburgh, PA, 1998.

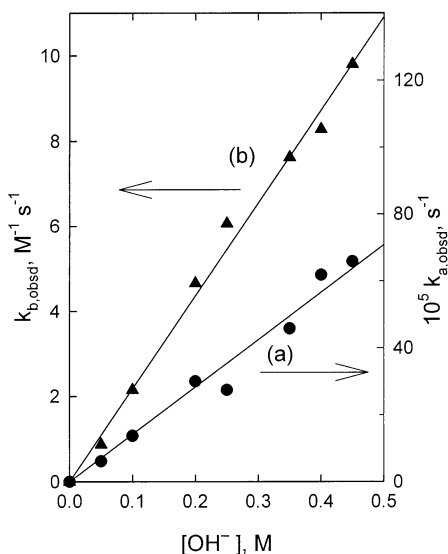


Figure 2. Dependence of the observed rate constants on $[\text{OH}^-]$: (a) $k_{a,\text{obsd}}$; (b) $k_{b,\text{obsd}}$. Conditions: 0.37 mM ClO_2 ; 0.05–0.45 M NaOH; 25.0(2) °C; $\mu = 1.0$ M. $k_a = 1.38(8) \times 10^{-3} \text{ M}^{-1} \text{ s}^{-1}$, and $k_b = 21.8(4) \text{ M}^{-2} \text{ s}^{-1}$.

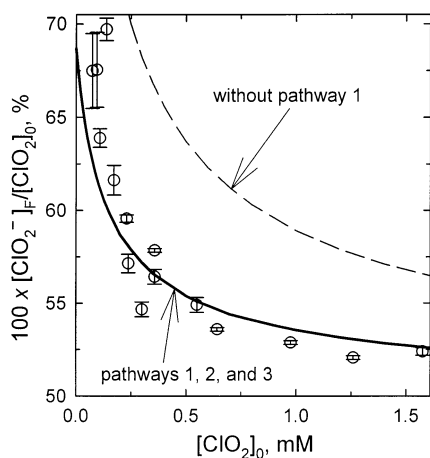
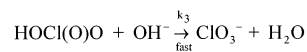
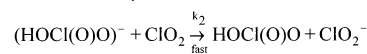
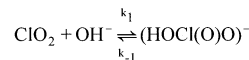


Figure 3. Effect of increasing $[\text{ClO}_2]_0$ on the $[\text{ClO}_2^-]_{\text{F}}/[\text{ClO}_2]_0$ ratio due to ClO_2 decomposition in basic solution (circles). Conditions: 0.05–1.58 mM ClO_2 ; 0.20 M NaOH. Predicted $[\text{ClO}_2^-]_{\text{F}}/[\text{ClO}_2]_0$ is based on the relative contribution from pathways 1 and 2 following eq 15 (solid line). $\alpha = 0.60(3)$, and $\beta = 0.40(2)$. The dashed line is the predicted $[\text{ClO}_2^-]_{\text{F}}/[\text{ClO}_2]_0$ ratio if only pathways 2 and 3 existed (eq 6, where k_a corresponds to pathway 2 only and k_b corresponds to pathway 3). The subscript F in $[\text{ClO}_2^-]_{\text{F}}$ refers to the final levels of chlorite formed upon the completion of the ClO_2 decay reaction.

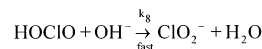
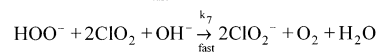
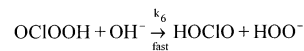
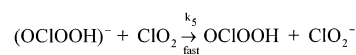
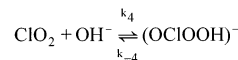
authors.^{8,10,12} As shown in Figure 3, the percent yield of ClO_2^- becomes greater than that of ClO_3^- as the concentration of ClO_2 decreases. At 74 μM ClO_2 , the ClO_2^- yield is 67.5% of the chlorine-containing products while the ClO_3^- yield is only 32.5%. As will be shown, there is a need to introduce three pathways to account for all products formed. It is clear that something must be oxidized to balance the excess reduction to ClO_2^- , and oxidation of water is the only possibility. Therefore, we propose the formation of O_2 (eq 3), a reaction that is thermodynamically very favorable in basic solution. The oxidation of water would proceed via peroxide intermediates, and it is known that HO_2^- reacts rapidly with ClO_2 to form O_2 and ClO_2^- .²² To eliminate other possible pathways, we also tested to see if any OCl^- is

Scheme 1. Proposed Mechanism for the Decomposition of Chlorine Dioxide in Basic Solution

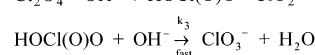
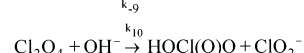
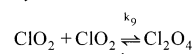
Pathway 1. First-order in $[\text{ClO}_2]$; products: $[\text{ClO}_2^-] = [\text{ClO}_3^-]$.



Pathway 2. First-order in $[\text{ClO}_2]$; products: ClO_2^- and O_2 .



Pathway 3. Second-order in $[\text{ClO}_2]$; products: $[\text{ClO}_2^-] = [\text{ClO}_3^-]$.



formed during ClO_2 decomposition. A flow-through apparatus allowed a continuous stream of $\text{ClO}_2(\text{g})$ to bubble slowly through a flask containing 0.20 M NaOH. This procedure allowed the ClO_2 that decomposed to be replenished and maintained a ClO_2 concentration of 0.10(2) mM in solution. Spectrophotometric analysis at two wavelengths (molar absorptivities ($\text{M}^{-1} \text{ cm}^{-1}$) at 260 nm are $\epsilon_{\text{OCl}^-} = 87.9$ and $\epsilon_{\text{ClO}_2^-} = 154$, and at 295 nm $\epsilon_{\text{OCl}^-} = 356$ and $\epsilon_{\text{ClO}_2^-} = 125$) was used to determine whether OCl^- was present. No OCl^- could be detected ($< 1 \mu\text{M}$) under conditions where 0.57(1) mM ClO_2^- formed. Ion chromatographic results for these conditions show that 0.560(4) mM ClO_2^- and 0.436(5) mM ClO_3^- formed. The values obtained by the ion chromatographic method are more precise than those determined using spectrophotometry and are in agreement within the error.

Low concentrations of ClO_2 favor ClO_2^- as a product compared to nearly equimolar levels of ClO_2^- and ClO_3^- formed at high ClO_2 concentrations. This suggests that the second-order pathway, which is preferred at higher concentrations, is responsible for the products in eq 1. However, the second-order pathway is not sufficient to account for all the chlorate formed. This indicates the presence of two pathways with a first-order dependence in ClO_2 , one produces equal amounts of ClO_2^- and ClO_3^- and the other forms ClO_2^- and O_2 . The product distribution is not affected by changes of OH^- concentration because all pathways have first-order dependence in $[\text{OH}^-]$.

Mechanism. Scheme 1 shows the proposed mechanism with three concurrent pathways needed to account for the kinetic and stoichiometric results. Pathway 1 generates a species where OH^- adducts to the Cl atom of ClO_2 to form an $(\text{HOCl}(\text{O})\text{O})^-$ intermediate. This is similar to adducts proposed for ClO_2 reactions with HO_2^- ,²³ I^- ,²⁴ and $\text{S}_2\text{O}_3^{2-}$.²⁵

(22) Hoigné, J.; Bader, H. *Water Res.* **1994**, 28, 45–55.

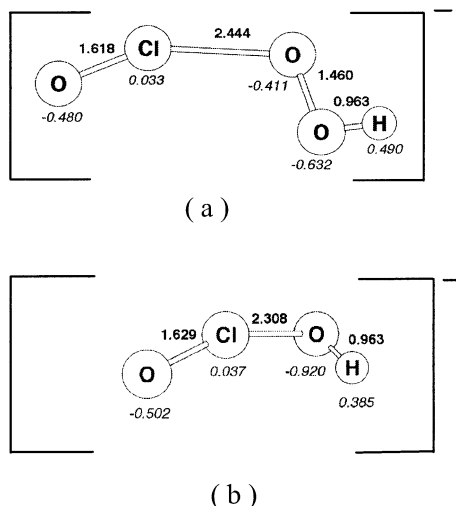
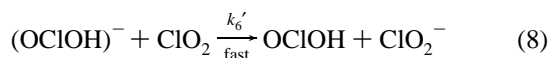
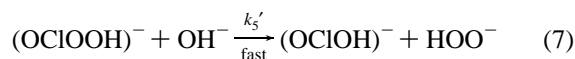


Figure 4. Equilibrium geometries (bond distances in Å) and atomic charges for the steady-state species (a) $(\text{OCIOOH})^-$ and (b) $(\text{OCIOH})^-$. The numbers are reported for the B3LYP/6-311++G(3df,3pd) level of theory.

An ab initio calculation for the $(\text{HOCl}(\text{O})\text{O})^-$ adduct¹⁴ shows a weak, but significant, interaction between Cl and the OH group. The subsequent electron-transfer step (k_2) is very rapid and generates ClO_2^- and HOClO_2 (which reacts rapidly with OH^- (k_3) to give ClO_3^-). Hence, the reaction is first order in $[\text{ClO}_2]$ and $[\text{OH}^-]$ and forms equimolar ClO_2^- and ClO_3^- . The reactions in the k_1 and k_2 steps can be considered as an example of base-assisted electron transfer.¹⁴

In pathway 2 we propose OH^- forms an adduct to one of the oxygen atoms of ClO_2 to give $(\text{OCIOOH})^-$ (k_4) as a reactive intermediate. An ab initio calculation of this species (Figure 4a) indicates a favorable intermediate where an OCl segment with a net charge of -0.447 is weakly bound to an OOH segment with net charge of -0.553 . This adduct can undergo rapid electron transfer with a second ClO_2 (k_5) to give ClO_2^- and OCIOOH . The latter species reacts favorably with OH^- to generate HOClO and HOO^- (k_6). The reaction between HOO^- and ClO_2 is known to give ClO_2^- and O_2 , where k_7 represents a series of rapid steps.²² The stoichiometry for the overall reaction in pathway 2 is given in eq 3, where no ClO_3^- is formed. The reactions in the k_4 and k_5 steps can be considered as another example of a base-assisted electron-transfer process. Alternative steps for the reaction of $(\text{OCIOOH})^-$ that lead to the same products are given in eqs 7 and 8. Ab initio calculations show that $(\text{OCIOH})^-$ is a possible intermediate (Figure 4b).



Pathway 3 is second-order in ClO_2 and proceeds via a Cl_2O_4 intermediate that is in rapid preequilibrium with two ClO_2 molecules (k_9/k_{-9}). This intermediate was proposed by Halperin and Taube⁹ and is similar to the proposed BrO_2^-

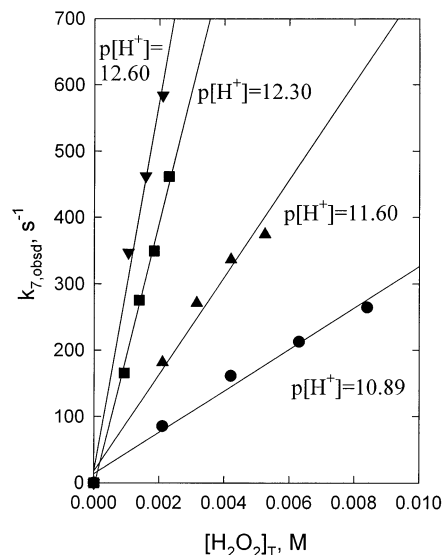
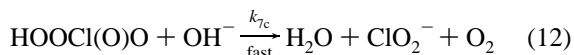
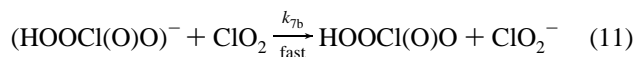


Figure 5. Effect of increasing $[\text{H}_2\text{O}_2]_{\text{T}}$ on the rate of the $\text{ClO}_2/\text{HO}_2^-$ reaction in the $\text{p}[\text{H}^+]$ range 10.89 to 12.60. The reaction was followed at 359 nm, 25.0 °C, $\mu = 1.0$ M, and 0.050 mM ClO_2 . $k_{7a} = 1.6(3) \times 10^5 \text{ M}^{-1} \text{ s}^{-1}$.

ClO_2 ¹⁴ and Br_2O_4 ²⁶ intermediates. Ab initio calculations have been reported previously¹⁶ for Cl_2O_4 . The reaction of Cl_2O_4 with OH^- in step k_{10} is another example of base-assisted electron transfer, in this case between two weakly associated ClO_2 molecules.

Hydrogen Peroxide Reaction with ClO_2 . Hoigné²² assigned a rate constant of $1.3(2) \times 10^5 \text{ M}^{-1} \text{ s}^{-1}$ for the reaction between HOO^- and ClO_2 in the pH range 5–11 (temperature and other conditions were not specified). We measured the rate by stopped-flow methods from $\text{p}[\text{H}^+] = 9.4$ to 12.6 by observing the loss of ClO_2 under pseudo-first-order conditions where $[\text{H}_2\text{O}_2]_{\text{T}} \gg [\text{ClO}_2]$. Figure 5 shows the dependence of $k_{7,\text{obsd}} (=k_{7a}[\text{HO}_2^-])$ on $[\text{H}_2\text{O}_2]_{\text{T}}$ at several $\text{p}[\text{H}^+]$ values. The rate expression is given in eq 9, where $[\text{H}_2\text{O}_2]_{\text{T}} = [\text{H}_2\text{O}_2] + [\text{HOO}^-]$ and k_{7a} is the rate-determining step for the reaction sequence given in eqs 10–12. Our value of $1.6(3) \times 10^5 \text{ M}^{-1} \text{ s}^{-1}$ for k_{7a} , at 25.0 °C and 1.0 M ionic strength, where $K_{\text{a}}^{\text{H}_2\text{O}_2}$ is $10^{-12.13} \text{ M}$,²⁷ is in good agreement with Hoigné's value. The reaction is independent of carbonate and phosphate (up to 80 mM) buffer concentrations. The k_{7a} rate constant for the HOO^- reaction is 9 orders of magnitude greater than the k_4 rate constant in pathway 2 and therefore does not affect the reaction rate between ClO_2 and OH^- .

$$\frac{-d[\text{ClO}_2]}{dt} = \left(\frac{2k_{7a}K_{\text{a}}^{\text{H}_2\text{O}_2}}{K_{\text{a}}^{\text{H}_2\text{O}_2} + [\text{H}^+]} \right) [\text{H}_2\text{O}_2]_{\text{T}}[\text{ClO}_2] \quad (9)$$



(23) Ni, Y.; Wang, X. *Can. J. Chem. Eng.* **1996**, *75*, 31–36.

(24) Fabian, I.; Gordon, G. *Inorg. Chem.* **1997**, *36*, 2494–2497.

(25) Horváth, A. K.; Nagypál, I. *J. Phys. Chem. A* **1998**, *102*, 7267–7272.

(26) Buxton, G. V.; Dainton, F. R. S. *Proc. R. Soc. A* **1968**, *304*, 427–439.

(27) Smith, R. M.; Martell, A. E. *Critical Stability Constants. Volume 4: Inorganic Complexes*; Plenum Press: New York, 1979; p 75.

Table 1. Summary of Rate Constants and Activation Parameters for the Decomposition of ClO₂ in Basic Solution

basic nucleophile	rate const ^a	ΔH^\ddagger , kJ mol ⁻¹	ΔS^\ddagger , J mol ⁻¹ K ⁻¹
OH ⁻	$k_a = 1.38(8) \times 10^{-3} \text{ M}^{-1} \text{ s}^{-1}$	60(2)	-101(6)
	$k_b = 21.8(4) \text{ M}^{-2} \text{ s}^{-1}$	32(2)	-119(7)
	$k_1 = 4.1(1) \times 10^{-4} \text{ M}^{-1} \text{ s}^{-1}$		
	$k_4 = 1.4(1) \times 10^{-4} \text{ M}^{-1} \text{ s}^{-1}$		
CO ₃ ²⁻	$(k_9/k_{-9})k_{10} = 10.9(2) \text{ M}^{-2} \text{ s}^{-1}$		
	$k_a^{\text{CO}_3} = 8.6(4) \times 10^{-4} \text{ M}^{-1} \text{ s}^{-1}$		
PO ₄ ³⁻	$k_b^{\text{CO}_3} = 6.7(2) \text{ M}^{-2} \text{ s}^{-1}$		
	$k_a^{\text{PO}_4} = 2.8(6) \times 10^{-5} \text{ M}^{-1} \text{ s}^{-1}$		
	$k_b^{\text{PO}_4} = 24(2) \text{ M}^{-2} \text{ s}^{-1}$		

^a Conditions: 25.0 °C; $\mu = 1.0 \text{ M NaClO}_4$; $\lambda = 359 \text{ nm}$.

Detailed Rate Expressions and Resolved Rate Constants. As the mechanism in Scheme 1 indicates, two ClO₂ radicals are consumed in pathways 1 and 3 while four are consumed in pathway 2. The rate expression in eq 13

$$-\frac{d[\text{ClO}_2]}{dt} = 2[\text{OH}^-][\text{ClO}_2] \left(\frac{k_1 k_2 [\text{ClO}_2]}{k_{-1} + k_2 [\text{ClO}_2]} + \frac{2k_4 k_5 [\text{ClO}_2]}{k_{-4} + k_5 [\text{ClO}_2]} + \frac{k_9 k_{10} [\text{ClO}_2]}{k_{-9} + k_{10} [\text{OH}^-]} \right) \quad (13)$$

$$-\frac{d[\text{ClO}_2]}{dt} = 2(k_1 + 2k_4)[\text{OH}^-][\text{ClO}_2] + \frac{2k_9 k_{10}}{k_{-9}} [\text{OH}^-][\text{ClO}_2]^2 \quad (14)$$

accounts for these stoichiometric factors and is derived on the basis of the assumption that (HOClO₂)⁻, (OClOOH)⁻, and Cl₂O₄ are each steady-state intermediates. If $k_{-1} \ll k_2$, $k_{-4} \ll k_5$, and $k_{-9} \gg k_{10}$, the rate expression is simplified to eq 14 that agrees with our experimental observations. The agreement between the experimental data and the fit down to micromolar levels of ClO₂ (Figure 1, insert) suggests that values for k_2/k_{-1} and k_5/k_{-4} are larger than 10^6 M^{-1} . As seen from eqs 6 and 14, the first-order rate constant (k_a) obtained from kinetic data equals $2(k_1 + 2k_4)$ and the second-order rate constant (k_b) equals $2k_9 k_{10}/k_{-9}$. Yields of ClO₂⁻ and ClO₃⁻ as a function of [ClO₂] are needed to resolve the k_1 and k_4 values. A total of 15 sets of reactions with [ClO₂]₀ varying from 0.074 to 1.58 mM in 0.20 M [OH⁻] were analyzed for ClO₂⁻ and ClO₃⁻ after 99.9% completion. Figure 3 shows the percent [ClO₂⁻]_F/[ClO₂]₀ as a function of the initial ClO₂ concentration. To resolve k_1 and k_4 values, kinetic traces were generated on the basis of eq 6 for the conditions in Figure 3. These traces were divided into 20 s intervals, and the amounts of ClO₂⁻ and ClO₃⁻ formed at the midpoint of each interval were calculated by successive approximation for 3000 data points. The summation of ClO₂⁻ formed at each time interval to give [ClO₂⁻]_F is expressed by eq 15, where α and β are the relative contributions of pathways 1 and 2, respectively, m is the interval number, and n is the total number of intervals. Similarly, the [ClO₃⁻]_F is given by eq 16, which needs only the α value. The value of 0.5 in these equations corresponds to the disproportionation reactions

(pathways 1 and 3), where half of the ClO₂ lost forms ClO₂⁻ and half forms ClO₃⁻. The regression analysis gives $\alpha = 0.60(3)$ and $\beta = 0.40(2)$. The solid line in Figure 3 shows the fit of the experimental data to eq 15 (after multiplying by 100/[ClO₂]₀) and corresponds to $k_1 = 4.1(4) \times 10^{-4} \text{ M}^{-1} \text{ s}^{-1}$ and $k_4 = 1.4(1) \times 10^{-4} \text{ M}^{-1} \text{ s}^{-1}$ (Table 1). The dashed line shows that pathways 2 and 3 alone are not sufficient to account for the observed [ClO₂⁻]_F/[ClO₂]₀ ratio (eq 6, where k_a corresponds to pathway 2 only and k_b corresponds to pathway 3).

$$[\text{ClO}_2^-]_F = \sum_{m=1}^n \left(\frac{0.5(\alpha k_a + k_b([\text{ClO}_2]_{20m} + [\text{ClO}_2]_{20m-20})/2) + \beta k_a}{k_a + k_b([\text{ClO}_2]_{20m} + [\text{ClO}_2]_{20m-20})/2} \right) \times ([\text{ClO}_2]_{20m-20} - [\text{ClO}_2]_{20m}) \quad (15)$$

$$[\text{ClO}_3^-]_F = \sum_{m=1}^n \left(\frac{0.5(\alpha k_a + k_b([\text{ClO}_2]_{20m} + [\text{ClO}_2]_{20m-20})/2)}{k_a + k_b([\text{ClO}_2]_{20m} + [\text{ClO}_2]_{20m-20})/2} \right) \times ([\text{ClO}_2]_{20m-20} - [\text{ClO}_2]_{20m}) \quad (16)$$

Temperature Dependence. The decomposition reactions of 0.10 mM ClO₂ in 0.20 M NaOH at $\mu = 1.0 \text{ M}$ were measured from 0.0 to 25.0 °C to resolve activation parameters for the composite rate constants, k_a and k_b (eq 6). The ΔH^\ddagger values, 60(2) kJ mol⁻¹ for k_a and 32(2) kJ mol⁻¹ for k_b , are in substantial agreement with previous values.¹⁰ The ΔS^\ddagger values are -101(6) J mol⁻¹ K⁻¹ for k_a and -119(7) J mol⁻¹ K⁻¹ for k_b . The large negative ΔS^\ddagger values for k_a ($=2k_1 + 4k_4$) and for k_b ($=2k_9 k_{10}/k_{-9}$) are consistent with the need to bring together several species in these composite rate constants. Eyring plots are given in Figure S3 (Supporting Information).

Buffer Effects. Basic carbonate and phosphate buffers accelerate the rate of ClO₂ decay, and the corresponding rate expressions are given in eq 17, where B = CO₃²⁻ or PO₄³⁻.

$$-\frac{d[\text{ClO}_2]}{dt} = k_a^{\text{B}}[\text{B}][\text{ClO}_2] + k_b^{\text{B}}[\text{B}][\text{ClO}_2]^2 \quad (17)$$

We found no contribution from HCO₃⁻ or HPO₄⁻ to the rate of ClO₂ decay. Figure 6 shows the significant contribution of CO₃²⁻ to both the first-order path ($k_a^{\text{CO}_3} = 8.6(4) \times 10^{-4} \text{ M}^{-1} \text{ s}^{-1}$) and the second-order path ($k_b^{\text{CO}_3} = 6.7(2) \text{ M}^{-2} \text{ s}^{-1}$), where $k_{a,\text{obsd}}^{\text{B}} = k_a^{\text{B}}[\text{B}]$ and $k_{b,\text{obsd}}^{\text{B}} = k_b^{\text{B}}[\text{B}]$. By contrast, previous evaluation¹⁰ gave $k_a^{\text{CO}_3} = 7 \times 10^{-14} \text{ M}^{-1} \text{ s}^{-1}$ (a value too low to be measured) and $k_b^{\text{CO}_3} = 2.45 \text{ M}^{-2} \text{ s}^{-1}$. The rate constants for PO₄³⁻ (Figure S4) are $k_a^{\text{PO}_4} = 2.8(6) \times 10^{-5} \text{ M}^{-1} \text{ s}^{-1}$ and $k_b^{\text{PO}_4} = 24(2) \text{ M}^{-2} \text{ s}^{-1}$. In these studies, contributions from the OH⁻ path were also observed with [OH⁻] = 6.3 × 10⁻³ M and were taken into account. Product studies in both buffers (Table 2) show that the percent of ClO₂⁻ formed increases as the concentration of ClO₂ decreases. This suggests that pathways analogous to pathway 2 also occur with carbonate and phosphate forming adducts

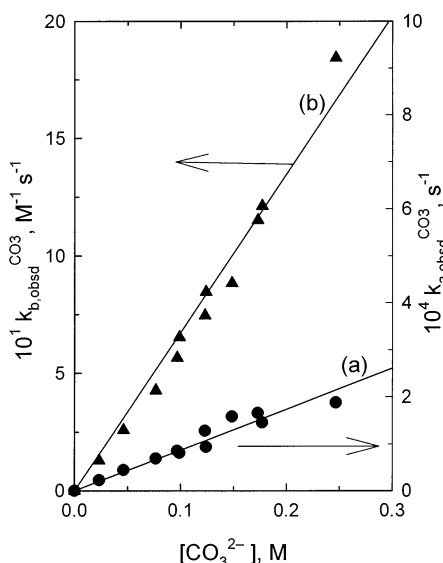


Figure 6. Dependence of (a) $k_{a,obsd}^{CO_3}$ and (b) $k_{b,obsd}^{CO_3}$ on $[CO_3^{2-}]$ for ClO_2 decomposition in basic solution. Conditions: 0.2 mM ClO_2 ; 20–250 mM CO_3^{2-} ; $p[H^+] = 9.4$ – 10.3 ; 25.0 °C; $\mu = 1.0$ M. $k_a^{CO_3} = 8.6(4) \times 10^{-4} M^{-1} s^{-1}$, and $k_b^{CO_3} = 6.7(2) M^{-2} s^{-1}$.

Table 2. Products of ClO_2 Decomposition in the Presence of (a) Carbonate and (b) Phosphate Buffer

$[ClO_2]_0, \mu M$	$[ClO_2^-]_F, \mu M$	$[ClO_3^-]_F, \mu M$	$100[ClO_2^-]_F/[ClO_2]_0, \%$
(a) Decomposition of ClO_2 in Carbonate Buffer ^{a-c}			
43.0(6)	26.4(3)	16.6(5)	61(1)
69.6(6)	39.6(3)	30.0(5)	56.9(7)
83.0(4)	47.2(2)	35.8(4)	56.9(4)
124.2(7)	68.8(2)	55.4(7)	55.4(4)
167.4(3)	90.4(3)	77.00(8)	54.0(2)
217(1)	115.4(2)	101(1)	53.2(3)
256.4(5)	138.4(3)	118.0(4)	54.0(2)
(b) Decomposition of ClO_2 in Phosphate Buffer ^{b-d}			
50.6(7)	32.6(1)	18.0(6)	64.4(9)
76.4(9)	46.2(2)	30.2(8)	60.5(7)
90.0(6)	57.8(2)	32.2(5)	64.2(4)
131.8(7)	75.6(5)	56.2(5)	57.4(5)
164(1)	91(2)	72.6(6)	56(1)
210(1)	119.0(7)	91.4(8)	56.6(4)
248(1)	135.0(6)	113.4(9)	54.3(4)

^a $[CO_3]_T = 0.10$ M; $p[H^+] = 10.2(1)$; $pK_a(HCO_3^-) = 9.48$; 25.0 °C. ^b The error represents the standard deviation of at least three runs for each sample analyzed. ^c The subscript F in $[ClO_2^-]_F$ and $[ClO_3^-]_F$ refers to the final levels of chlorite and chlorate formed upon the completion of the ClO_2 decay reaction. ^d $[PO_4]_T = 0.10$ M; $p[H^+] = 11.8(1)$; $pK_a(HPO_4^{2-}) = 11.08$; 25.0 °C.

with ClO_2 (i.e. $(OCIOOCO_2)^{2-}$ and $(OCIOOPO_3)^{3-}$ species). The ratios of k_a/k_b rate constants for these bases are 1.28×10^{-4} M for CO_3^{2-} , 6.33×10^{-5} M for OH^- , and 1.1×10^{-6} M for PO_4^{3-} . Thus, the first-order pathways are more favorable for CO_3^{2-} than for OH^- and are less favorable for PO_4^{3-} .

Comparison of the Reactions of ClO_2/ClO_2 , ClO_2/BrO_2 , and BrO_2/BrO_2 in Base. The decomposition kinetics of ClO_2 require basic nucleophiles (CO_3^{2-} , PO_4^{3-} , and OH^-) for both the first-order and the second-order pathways, whereas a much broader group of nucleophiles (that include Cl^- , Br^- , ClO_2^- , SO_4^{2-} , CH_3COO^- , and HPO_4^{2-} as well as CO_3^{2-} , PO_4^{3-} , and OH^-) assists the electron-transfer reactions between ClO_2 and BrO_2 .¹⁴ Both the ClO_2/ClO_2 and ClO_2/BrO_2 reactions consume base and become much more

Table 3. Comparison of the Rate Constants for Cl_2O_4 , ClO_2BrO_2 , and Br_2O_4 Reactions with OH^-

reacn	$K_9 k_{10}, M^{-2} s^{-1} a$
$2ClO_2 + OH^- \rightarrow ClO_2^- + HOClO_2$	10.9 ^b
$ClO_2 + BrO_2 + OH^- \rightarrow BrO_2^- + HOClO_2$	1.25×10^8 ^c
$2BrO_2 + OH^- \rightarrow BrO_2^- + HOBrO_2$	1.3×10^{13} ^{d,e}

^a $K_9 = k_9/k_{-9}$. ^b This work. ^c Reference 14. ^d Reference 26. ^e Reference 28.

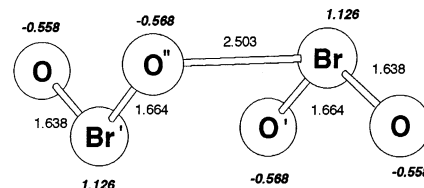
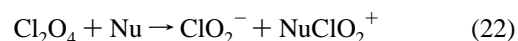
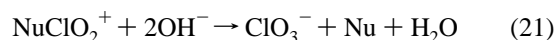
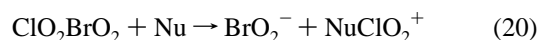
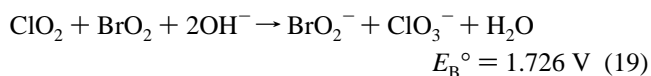
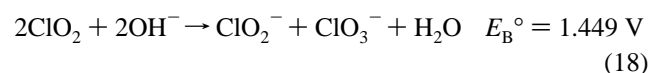


Figure 7. Equilibrium geometries (bond distances in Å) and atomic charges (italics) for $OBrOBr(O)O$. The numbers are reported for the B3LYP/6-311++G(3df,3pd) level of theory.

favorable thermodynamically as the hydroxide ion concentration increases as shown by the redox potentials in eqs 18 and 19. The reactions of nucleophiles (Nu) with ClO_2/BrO_2 have been proposed¹⁴ to first generate $NuClO_2^+$ and BrO_2^- (eq 20). These $NuClO_2^+$ species then react with OH^- to give ClO_3^- and release Nu (eq 21). A similar process for Cl_2O_4 would correspond to eq 22, which would be followed by a step analogous to eq 21. However, the reaction in eq 22 is thermodynamically less favorable than that in eq 20 because the reduction potential for BrO_2/BrO_2^- is favored over that of ClO_2/ClO_2^- by 0.28 V. The intermediate $NuClO_2^+$ in eq 22 appears to be more difficult to form unless Nu is a strong base.



Third-order rate constants ($M^{-2} s^{-1}$) for reactions of the halogen dioxides with OH^- (Table 3) increase by 12 orders of magnitude for the following sequence: $ClO_2 + ClO_2$;¹⁶ $ClO_2 + BrO_2$;¹⁴ $BrO_2 + BrO_2$.^{26,28,29} Much of this enormous change in reactivity can be attributed to the relative stabilities of Cl_2O_4 ,¹⁶ ClO_2BrO_2 ,¹⁴ and Br_2O_4 (Figure 7, Table S6), where the association constants of the halogen dioxide increase by a factor of 3×10^5 from Cl_2O_4 to Br_2O_4 on the basis of our ab initio calculations. The relative rate of OH^- reaction with the halogen dioxide dimers increases greatly from Cl_2O_4 to Br_2O_4 .

(28) Field, J. R.; Försterling, H.-D. *J. Phys. Chem.* **1986**, *90*, 5400–5407.
(29) Nicoson, J. S.; Wang, L.; Becker, R. H.; Huff Hartz, K. E.; Muller, C. E.; Margerum, D. W. *Inorg. Chem.* **2002**, *41*, 2975–2980.

Deviation from Marcus Theory. An alternative possibility for pathway 1 is a direct electron transfer between ClO_2 and OH^- to form ClO_2^- and OH . A subsequent reaction of OH and ClO_2 would give HClO_3 . Table S3 gives rate constants determined for the reaction of ClO_2 with OH^- and HO_2^- (k_{meas}) as well as the electron-transfer reactions of ClO_2 with NO_2^- ,³⁰ N_3^- ,³¹ SO_3^{2-} ,³² and SCN^- ³³ on the basis of Marcus theory.³⁴ Self-exchange rate constants³⁵ and redox potentials³⁶ have been compiled by Stanbury. The measured rate constant for the ClO_2/OH^- reaction ($k_{\text{meas}} = k_1$) is 2×10^4 times larger than expected by Marcus theory. Previous studies have discussed inner-sphere mechanisms, orbital overlap of reactants, and solvent nonadditivity as factors

- (30) Stanbury, D. M.; Martinez, R.; Tseng, E.; Miller, C. E. *Inorg. Chem.* **1988**, *27*, 4277–4280.
 (31) Awad, H. H.; Stanbury, D. M. *J. Am. Chem. Soc.* **1993**, *115*, 3636–3642.
 (32) Suzuki, K.; Gordon, G. *Inorg. Chem.* **1978**, *17*, 3115–3118.
 (33) Figler, J. N.; Stanbury, D. M. *J. Phys. Chem. A* **1999**, *103*, 5732–5741.
 (34) Espenson, J. H. *Chemical Kinetics and Reaction Mechanisms*, 2nd ed.; McGraw-Hill: New York, 1995; pp 243–247.
 (35) Stanbury, D. M. *Advances in Chemistry Series: Electron-Transfer Reactions*; American Chemical Society: Washington, DC, 1997; pp 165–182.
 (36) Stanbury, D. M. *Advances in Inorganic Chemistry*; Academic: New York, 1989; Vol. 33, pp 69–138.

responsible for the large deviation from the traditional Marcus theory in the case of small molecules.³¹ We propose that the large deviation from the Marcus theory is an indication that the measured rate constants represent adduct formation reactions rather than actual electron-transfer processes. The mechanism proposed in Scheme 1 shows that the adduct in k_1 has to form first for the electron transfer in k_2 to take place. Pathways 2 and 3 also involve adduct formation followed by electron transfer. In the case of HOO^- , a similar mechanism is shown in eqs 10 and 11 and is in agreement with the proposed mechanism by Ni and Wang.²³ Recent work in the Margerum group¹⁴ has shown that when ClO_2 reacts with BrO_2 , an adduct formation with a nucleophile is needed first to allow an electron-transfer process to occur.

Acknowledgment. This work was supported by National Science Foundation Grants CHE-9818214 and CHE-0139876.

Supporting Information Available: Tables and figures with supplemental kinetic and product data, the derivation of eq 5, and the detailed method for use of eqs 15 and 16. This material is available free of charge via the Internet at <http://pubs.acs.org>.

IC0204676